

## Synthesis, single crystal X-ray diffraction, Hirshfeld surface and biological activity of quinolone derivatives

Huma Bano <sup>1</sup>, Sarah Shafi <sup>1</sup>, Hina Siddiqui <sup>1</sup>, Muhammad Iqbal Choudhary <sup>1,2</sup> and Sammer Yousuf <sup>1,\*</sup>

<sup>1</sup> H.E.J. Research Institute of Chemistry, International Center for Chemical and Biological Sciences, University of Karachi, Karachi-75270, Pakistan

<sup>2</sup> Department of Biochemistry, Faculty of Science, King Abdulaziz University, Jeddah-21412, Kingdom of Saudi Arabia

\* Corresponding author at: H.E.J. Research Institute of Chemistry, International Center for Chemical and Biological Sciences, University of Karachi, Karachi-75270, Pakistan.

Tel.: +92.21.34824924-5. Fax: +92.21.4819018-9. E-mail address: [dr.sammer.yousuf@gmail.com](mailto:dr.sammer.yousuf@gmail.com) (S. Yousuf).

### ARTICLE INFORMATION



DOI: 10.5155/eurjchem.8.4.422-429.1651

Received: 10 September 2017

Received in revised form: 19 September 2017

Accepted: 20 September 2017

Published online: 31 December 2017

Printed: 31 December 2017

### KEYWORDS

Multi-drug resistance  
 Quinolone derivatives  
 Anti-bacterial activity  
 X-ray crystallography  
 Antileishmanial activity  
 Hirshfeld surface analysis

### ABSTRACT

Two new quinolone derivatives, 5-nitroquinolin-8-yl-3-bromobenzoate (1) and 5-nitroquinolin-8-yl-3-chlorobenzoate (2), were synthesized and their structures were elucidated using X-ray diffraction techniques. Both compounds crystallized in  $P2_1/n$  (monoclinic) space group having four independent molecules in asymmetric unit. The dihedral angle between benzene and planar quinoline rings in compounds 1 and 2 were found to be  $117.7(2)$  and  $117.4(2)^\circ$ , respectively. No intermolecular hydrogen bonding was observed in compound 1. However, C-H...O intermolecular interaction was found to connect the molecules in crystal lattice of compound 2. Hirshfeld surfaces analysis was performed to evaluate the directions, and strength of interactions of molecules of compounds and 1 and 2 with neighbouring molecules, and the major contribution in the crystal packing was due to O-H (1, 24.6% and 2, 25.1%) interactions. The synthesized quinolone derivatives were found as potent anti-bacterial agents against *E. coli* reference (ATCC25922 and ATCC 35218) and multi-drug resistant strains (M2 and M3) with 91.42 to 94.72% inhibition. Both compounds 1 and 2 showed weak antileishmanial activity against *L. Major* promastigotes *in vitro* with  $IC_{50}$  values  $73.2 \pm 3.1$  and  $72.2 \pm 2.3$   $\mu\text{g}/\text{mL}$ , respectively, and also found as cytotoxic in nature against 3T3 fibroblast cell line.

Cite this: *Eur. J. Chem.* 2017, 8(4), 422-429

### 1. Introduction

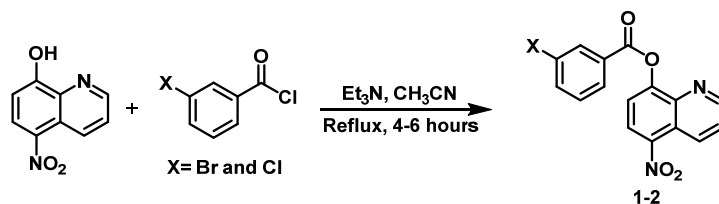
Quinolone, also known as benzopyridine, 1-benzazine, benzo[b]pyridine, or benzazine, is an aromatic heterocyclic compound having fused phenyl and pyridine moieties. Derivatives of quinolone have attracted attention of medicinal chemists due to their wide range of biological applications [1]. Among medicinally important heterocyclic compounds, quinolones are the most privileged class of compounds, as they are widely used as "parental" molecules to synthesize a broad range of biologically active molecules as anti-malarial [2], anti-cancer [3], anti-hypertensive [4], anti-TB [5], anti-inflammatory [6], and anti-HIV [7,8] agents. The wide range of biological activities prompted structural chemists to explore the substitution pattern of quinoline derivatives, which allows the large libraries of structurally diverse derivatives with interesting biological activities. Further to our interest in the synthesis of diverse biologically active derivatives of quinoline, we have synthesized 5-nitroquinolin-8-yl-3-bromobenzoate (1), and 5-nitroquinolin-8-yl-3-chlorobenzoate (2). Their structures were studied by using single crystal X-ray diffraction techniques, followed by detailed Hirshfeld quantitative analysis of contributions of various non-covalent interactions

towards the crystal stability in compounds 1 and 2. Both quinoline derivatives were also evaluated for their antileishmanial and anti-bacterial activity *in vitro* and interesting results were obtained. Both compounds were also checked for their cytotoxicity against 3T3 fibroblast cell line and found to be toxic in nature.

### 2. Experimental

#### 2.1. Materials, physical measurements and softwares

Analytical grade chemicals were purchased from Sigma-Aldrich. Single crystal X-ray diffraction data was collected by using  $\text{MoK}\alpha$  radiation ( $\lambda = 0.71073 \text{ \AA}$ ) on a Bruker SMART APEX-II diffractometer fitted with CCD detector at a temperature of  $273(2) \text{ K}$ . SAINT program was used to integrate the reflection intensities whereas, multi-scan method was used for absorption correction (SADABS) [9]. Finally the structures were constructed by using SHELXTL program [10,11]. PLATON calculations were used to find the significant non-covalent interactions in the molecule [12]. Quantitative analysis of intermolecular interactions was determined by using CIF file input in software package CrystalExplorer [13].



Scheme 1



Figure 1. The molecular structure of compounds 1 and 2.

Two-dimensional fingerprint plots were used to represent these interactions quantitatively using  $d_{\text{norm}}$  values by placing de versus  $d_i$ , in which cyan dots represent the area of the interaction towards the total Hirshfeld surface. MDR *Escherichia coli* strains (ATCC 35218 and ATCC 25922) were purchased from the American Type Cultures Center (ATCC). The duly characterized Pakistani multi-drug resistant clinical isolates of *E. coli* (M2 and M3, Source: Human urine) were obtained from the Diagnostic Laboratory of Liaquat National Hospital (LNH), Karachi, Pakistan. All the compounds were dissolved in DMSO with the ratio of 1:1 to prepare the stock solution.

### 2.2. X-ray structure determination

The constructed was solved and refined by direct and least-square methods, respectively [10,14]. All non-hydrogen atoms were refined on the basis of anisotropic thermal displacement parameters while hydrogen atoms were allowed to ride on calculated positions at parent atoms on the basis of isotropic thermal parameters.

### 2.3. Preparation of quinoline derivatives

Quinoline derivatives **1** and **2** were prepared by using the method as described by Moreno-Fuquen, and co-workers with slight modification [15]. 8-Hydroxy-5-nitroquinoline (1.0 mmol, 0.19 g) was dissolved in 10 mL acetonitrile. Triethyl amine (0.7 mmol, 0.1 mL) was added and mixture was refluxed for 15 minutes, followed by addition of acid halides (1.0 mmol, 0.21 g (**1**), 1.0 mmol (**2**) 0.17 g) and refluxed for 4 to 6 hours. Progress of the reaction was monitored through thin layer chromatography, after complete consumption of starting material, solvent was evaporated under reduced pressure. The crude product was washed with mixture of hexanes: ethyl acetate (v:v, 8:2), dried, and recrystallized from methanol (Scheme 1).

### 2.4. Evaluation of biological activities

Antileishmanial activity was performed by using method described by Choudhary and co-workers [16]. Anti-bacterial activity was performed by using methods previously described by Siddiqui and co-workers [17]. Whereas the cytotoxic activity was evaluated by using the MTT assay as explained by Oladimeji et al. [18].

## 3. Results and discussion

The molecular structures (Figure 1) and ORTEP diagrams of quinoline derivatives **1** and **2** are shown in Figures 2 and 3, respectively. Crystallographic data, selected bond lengths and angles, atomic displacement parameters, and hydrogen bond geometry are presented in Tables 1-6.

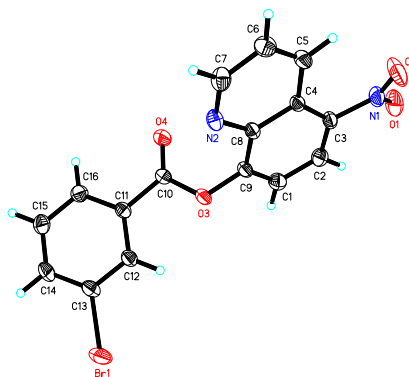


Figure 2. ORTEP view of single crystal structure of compound 1.

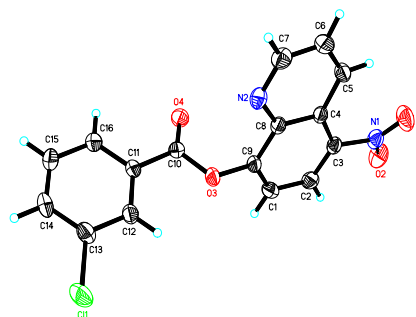


Figure 3. ORTEP view of single crystal structure of compound 2.

### 3.1. Structural features and crystal packing

The structures of compounds **1** and **2** were found to be composed of planner nitro-substituted quinoline ring system (C1/C7/N2/C9/C10) and planner bromo- and chloro-substi-

**Table 1.** Crystallographic data of compounds **1** and **2**.

Compound	1	2
Empirical formula	C <sub>16</sub> H <sub>9</sub> BrN <sub>2</sub> O <sub>4</sub>	C <sub>16</sub> H <sub>9</sub> ClN <sub>2</sub> O <sub>4</sub>
Formula weight	373.16	328.70
Temperature (K)	100 (2)	273 (2)
Crystal system	P2 <sub>1</sub> /n	P2 <sub>1</sub> /n
Space group	Monoclinic	Monoclinic
Hall symbol	-P 2yn	-P 2yn
a (Å)	6.5360 (4)	604835 (6)
b (Å)	16.2361 (11)	16.3002 (15)
c (Å)	13.6968 (8)	13.5332 (12)
β (°)	96.251(1)	95.264(2)
Volume (Å <sup>3</sup> )	1444.85 (16)	1424.2 (2)
Z	4	4
ρ <sub>calc</sub> (g/cm <sup>3</sup> )	1.715	1.533
F(000)	744	672
Crystal size (mm <sup>3</sup> )	0.51×0.39×0.28	0.32×0.23×0.13
Radiation	0.71073	0.71073
2θ range for data collection (°)	1.95 to 28.34	1.96 to 25.50
Index ranges	-8 ≤ h ≤ 8, -14 ≤ k ≤ 21, -18 ≤ l ≤ 15	-6 ≤ h ≤ 7, -16 ≤ k ≤ 19, -16 ≤ l ≤ 16
Radiation collected	10403	8330
Absorption correction	2.863	0.291
T <sub>min</sub> , T <sub>max</sub>	0.221, 0.570	0.912, 0.964
F(000)	744	672
Independent reflections	3606 [R <sub>int</sub> = 0.0279]	2647 [R <sub>int</sub> = 0.0372]
Data/restraints/parameters	3606 / 0 / 208	2647 / 0 / 208
Goodness of fit on F <sup>2</sup>	1.060	0.840
Final R indices [I > 2σ(I)]	R <sub>1</sub> = 0.0449, wR <sub>2</sub> = 0.1140	R <sub>1</sub> = 0.0435, wR <sub>2</sub> = 0.1022
R indices (all data)	R <sub>1</sub> = 0.0622, wR <sub>2</sub> = 0.1237	R <sub>1</sub> = 0.0761, wR <sub>2</sub> = 0.1272
Largest diff. peak / hole (eÅ <sup>-3</sup> )	0.420 and -1.131	0.299 and -0.222

**Table 2.** Selected bond lengths and angles of compound **1**.

Atom-Atom	Bond lengths [Å]	Atom-Atom	Bond lengths [Å]
Br(1)-C(14)	1.885 (2)	C(3)-C(4)	1.426(3)
O(3)-C(11)	1.365 (3)	C(4)-C(5)	1.412(3)
O(3)-C(10)	1.392(2)	C(4)-C(9)	1.426(3)
O(4)-C(11)	1.193(3)	C(9)-C(10)	1.415(3)
O(1)-N(1)	1.206(3)	C(13)-C(14)	1.378(3)
N(2)-C(7)	1.314(3)	C(10)-C(1)	1.350(3)
N(2)-C(9)	1.360(3)	C(16)-C(15)	1.370(4)
N(1)-O(2)	1.220(3)	C(16)-C(17)	1.388(3)
N(1)-C(3)	1.471(3)	C(5)-C(6)	1.357(4)
C(12)-C(13)	1.386(3)	C(14)-C(15)	1.385(4)
C(12)-C(17)	1.387(3)	C(2)-C(1)	1.401(3)
C(12)-C(11)	1.486(3)	C(7)-C(6)	1.400(4)
C(3)-C(2)	1.351(3)		
Atom-Atom-Atom	Bond angles [°]	Atom-Atom-Atom	Bond angles [°]
C(11)-O(3)-C(10)	117.66(17)	O(4)-C(11)-C(12)	125.6(2)
C(7)-N(2)-C(9)	117.4(2)	O(3)-C(11)-C(12)	110.90(17)
O(1)-N(1)-O(2)	122.6(2)	C(14)-C(13)-C(12)	119.0(2)
O(1)-N(1)-C(3)	118.8(2)	C(1)-C(10)-O(3)	118.4(2)
O(2)-N(1)-C(3)	118.5(2)	C(1)-C(10)-C(9)	122.6(2)
C(13)-C(12)-C(17)	120.1(2)	O(3)-C(10)-C(9)	118.8(2)
C(13)-C(12)-C(11)	121.23(19)	C(15)-C(16)-C(17)	120.9(2)
C(17)-C(12)-C(11)	118.61(19)	C(12)-C(17)-C(16)	119.6(2)
C(2)-C(3)-C(4)	122.7(2)	C(6)-C(5)-C(4)	119.7(2)
C(2)-C(3)-N(1)	116.0(2)	C(13)-C(14)-C(15)	121.5(2)
C(4)-C(3)-N(1)	121.2(2)	C(13)-C(14)-Br(1)	118.71(18)
C(5)-C(4)-C(9)	116.2(2)	C(15)-C(14)-Br(1)	119.77(17)
C(5)-C(4)-C(3)	127.5(2)	C(3)-C(2)-C(1)	120.5(2)
C(9)-C(4)-C(3)	116.30(19)	C(16)-C(15)-C(14)	118.9(2)
N(2)-C(9)-C(10)	117.81(19)	C(10)-C(1)-C(2)	119.0(2)
N(2)-C(9)-C(4)	123.4(2)	N(2)-C(7)-C(6)	123.6(2)
C(10)-C(9)-C(4)	118.83(19)	C(5)-C(6)-C(7)	119.6(2)
O(4)-C(11)-O(3)	123.49(19)		

tuted benzene rings (C11-C16) linked to each other by carboxylate bridges (C10/O3/O4), represented in [Figure 2](#) and [3](#). The dihedral angles between the planner quinoline and benzene rings were found to be 117.7(2) and 117.4 (2)° for compounds **1** and **2**, respectively.

In compound **1**, no inter- and intra-molecular hydrogen bondings were observed, and molecules were found to be arranged in three dimensions ([Figure 4](#)). Similarly in compound **2** no classical hydrogen bonding was observed. However, two neighboring molecules were found to be linked through C14-H14A...O1 intermolecular hydrogen bond with donor acceptor distance 3.4813 Å and angle of 16°, respectively. Molecules found to be arranged along *c*-axis ([Figure 5](#)).

### 3.2. Hirshfeld surface and fingerprint plot analysis

The quantitative Hirshfeld surface calculations to predict the directions and strength of interactions with neighboring molecules was carried both for compounds **1** and **2**. The circular red regions generated Hirshfeld indicated the strong O...H hydrogen-bonds that can be easily observed in compound **2** as compared to compound **1** ([Figure 6](#) and [7](#)). The two-dimensional fingerprint plot ([Figure 8](#) and [9](#)) of Hirshfeld of compounds **1** and **2** represent the percent contacts contributed towards crystal packing as depicted in [Figures 8](#) and [10](#) for compound **1** and [Figures 9](#) and [11](#) for compound **2**.

**Table 3.** Selected bond lengths and angles of compound 2.

Atom-Atom	Bond lengths [Å]	Atom-Atom	Bond lengths [Å]
O(3)-C(11)	1.365(3)	C(12)-C(13)	1.381(3)
O(3)-C(10)	1.394(3)	C(12)-C(17)	1.383(3)
C(4)-C(5)	1.415(3)	C(12)-C(11)	1.485(3)
C(4)-C(9)	1.420(3)	C(3)-C(2)	1.351(4)
C(4)-C(3)	1.425(3)	N(2)-C(7)	1.309(3)
O(4)-C(11)	1.188(3)	C(13)-C(14)	1.381(3)
C(10)-C(1)	1.348(4)	C(5)-C(6)	1.352(4)
C(10)-C(9)	1.409(3)	C(7)-C(6)	1.397(4)
C(9)-N(2)	1.366(3)	C(1)-C(2)	1.393(4)
N(1)-O(1)	1.218(3)	C(17)-C(16)	1.378(4)
N(1)-O(2)	1.219(3)	C(14)-C(15)	1.379(4)
N(1)-C(3)	1.477(3)	C(16)-C(15)	1.369(4)
Atom-Atom-Atom	Bond angles [°]	Atom-Atom-Atom	Bond angles [°]
C(11)-O(3)-C(10)	117.45(19)	C(2)-C(3)-N(1)	116.4(2)
C(5)-C(4)-C(9)	116.4(2)	O(4)-C(11)-O(3)	123.7(2)
C(5)-C(4)-C(3)	127.6(2)	O(4)-C(11)-C(12)	125.7(2)
C(9)-C(4)-C(3)	115.9(2)	O(3)-C(11)-C(12)	110.6(2)
C(1)-C(10)-O(3)	118.3(2)	C(7)-N(2)-C(9)	117.5(2)
C(1)-C(10)-C(9)	122.3(2)	C(14)-C(13)-C(12)	119.2(2)
O(3)-C(10)-C(9)	119.2(2)	C(6)-C(5)-C(4)	119.3(2)
N(2)-C(9)-C(10)	117.7(2)	N(2)-C(7)-C(6)	123.6(3)
N(2)-C(9)-C(4)	123.0(2)	C(10)-C(1)-C(2)	119.2(2)
C(10)-C(9)-C(4)	119.3(2)	C(16)-C(17)-C(12)	120.0(3)
O(1)-N(1)-O(2)	123.1(2)	C(3)-C(2)-C(1)	120.3(2)
O(1)-N(1)-C(3)	118.7(2)	C(15)-C(14)-C(13)	121.3(3)
O(2)-N(1)-C(3)	118.1(3)	C(15)-C(14)-Cl(1)	119.8(2)
C(13)-C(12)-C(17)	119.8(2)	C(13)-C(14)-Cl(1)	118.9(2)
C(13)-C(12)-C(11)	121.3(2)	C(5)-C(6)-C(7)	120.0(3)
C(17)-C(12)-C(11)	118.9(2)	C(15)-C(16)-C(17)	120.9(3)
C(2)-C(3)-C(4)	122.8(2)	C(16)-C(15)-C(14)	118.9(2)

**Table 4.** Anisotropic displacement parameters [Å<sup>2</sup>] for compound 1.

Atom	U <sup>11</sup>	U <sup>22</sup>	U <sup>33</sup>	U <sup>23</sup>	U <sup>13</sup>	U <sup>12</sup>
Br(1)	87 (1)	101 (1)	36 (1)	17 (1)	6 (1)	-28 (1)
O(3)	49 (1)	56 (1)	24 (1)	2 (1)	-3 (1)	-13 (1)
O(4)	52 (1)	58 (1)	38 (1)	11 (1)	2 (1)	-9 (1)
O(1)	58 (1)	75 (1)	74 (1)	12 (1)	-25 (1)	13 (1)
N(2)	43 (1)	39 (1)	41 (1)	2 (1)	-7 (1)	5 (1)
N(1)	41 (1)	59 (1)	43 (1)	9 (1)	-11 (1)	-3 (1)
C (12)	41 (1)	32 (1)	29 (1)	-4 (1)	1 (1)	-1 (1)
C (3)	36 (1)	42 (1)	33 (1)	4 (1)	-5 (1)	-4 (1)
C (4)	36 (1)	33 (1)	29 (1)	3 (1)	-1 (1)	-5 (1)
O (2)	82 (2)	120 (2)	50 (1)	-23 (1)	-27 (1)	21 (2)
C (9)	36 (1)	30 (1)	29 (1)	2 (1)	-2 (1)	-3 (1)
C (11)	40 (1)	38 (1)	29 (1)	-1 (1)	4 (1)	0 (1)
C (13)	44 (1)	40 (1)	30 (1)	0 (1)	-1 (1)	-4 (1)
C (10)	41 (1)	43 (1)	26 (1)	2 (1)	-1 (1)	-7 (1)
C (16)	46 (1)	63 (2)	43 (1)	-10 (1)	-5 (1)	-12 (1)
C (17)	44 (1)	50 (1)	37 (1)	-6 (1)	5 (1)	-9 (1)
C (5)	49 (1)	47 (1)	32 (1)	-6 (1)	1 (1)	-2 (1)
C (14)	57 (1)	41 (1)	31 (1)	2 (1)	1 (1)	-5 (1)
C (2)	34 (1)	56 (1)	48 (1)	2 (1)	2 (1)	7 (1)
C (15)	55 (1)	54 (1)	31 (1)	-3 (1)	-9 (1)	-2 (1)
C (1)	45 (1)	58 (2)	39 (1)	-5 (1)	8 (1)	2 (1)
C (7)	44 (1)	45 (1)	60 (2)	-5 (1)	-1 (1)	11 (1)
C (6)	55 (2)	52 (2)	48 (1)	-13 (1)	10 (1)	3 (1)

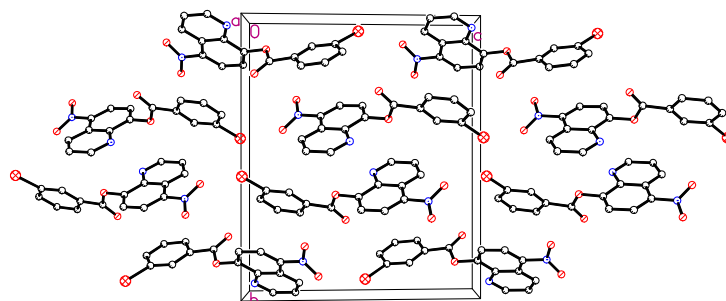
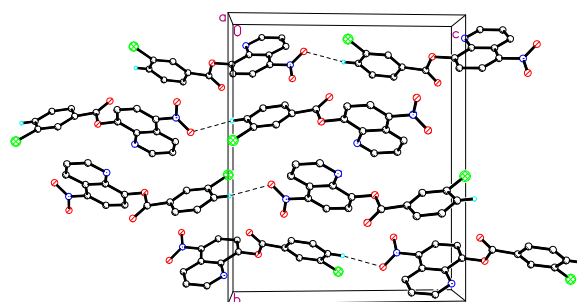
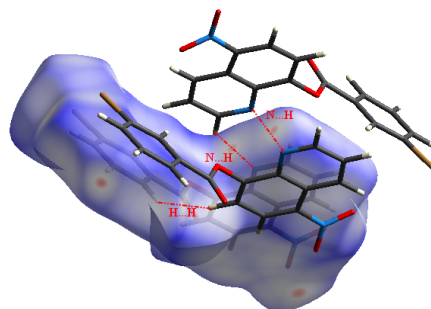
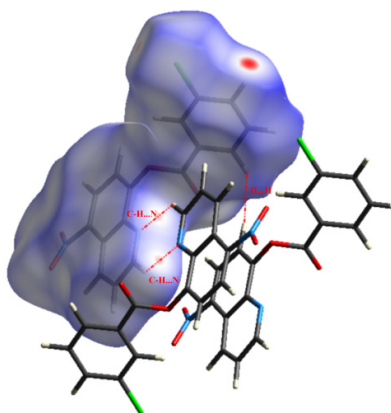
**Table 5.** Anisotropic displacement parameters [Å<sup>2</sup>] for the compound 2.

Atom	U <sup>11</sup>	U <sup>22</sup>	U <sup>33</sup>	U <sup>23</sup>	U <sup>13</sup>	U <sup>12</sup>
Cl(1)	110(1)	118 (1)	45 (1)	21 (1)	6 (1)	-32 (1)
O(3)	51(1)	65 (1)	31 (1)	5 (1)	-4 (1)	-14 (1)
C(4)	38(1)	40 (2)	36 (1)	3 (1)	-1 (1)	-8 (1)
O(4)	54(1)	65 (1)	43 (1)	11 (1)	3 (1)	-11 (1)
C(10)	41(1)	52 (2)	32 (1)	2 (1)	-2 (1)	-8 (1)
C(9)	37(1)	40 (1)	38 (1)	4 (1)	-1 (1)	-5 (1)
N(1)	45(1)	68 (2)	48 (1)	10 (1)	-10 (1)	-6 (1)
C(12)	43(1)	40 (1)	33 (1)	-4 (1)	1 (1)	1 (1)
C(3)	37(1)	49 (2)	39 (1)	7 (1)	-4 (1)	-6 (1)
C(11)	38 (1)	47 (2)	38 (1)	-1 (1)	4 (1)	1 (1)
N (2)	43 (1)	48 (1)	52 (1)	1 (1)	-8 (1)	3 (1)
O (2)	56 (1)	81 (2)	84 (2)	16 (1)	-24 (1)	10 (1)
C (13)	50 (2)	50 (2)	38 (1)	-2 (1)	-2 (1)	-6 (1)
C (5)	55 (2)	54 (2)	37 (1)	-4 (1)	2 (1)	-7 (1)
C (7)	47 (2)	49 (2)	70 (2)	-7 (2)	4 (1)	6 (1)
C (1)	48 (2)	66 (2)	41 (1)	-6 (1)	9 (1)	3 (1)
C (17)	49 (2)	59 (2)	43 (1)	-6 (1)	3 (1)	-8 (1)
C (2)	37 (1)	64 (2)	52 (2)	2 (1)	3 (1)	6 (1)
C (14)	69 (2)	54 (2)	38 (1)	4 (1)	2 (1)	-4 (1)
C (6)	55 (2)	59 (2)	58 (2)	-14 (1)	12 (1)	1 (1)
C (16)	50 (2)	78 (2)	50 (2)	-12 (2)	-8 (1)	-8 (2)
O (1)	80 (2)	115 (2)	53 (1)	-16 (1)	-23 (1)	11 (1)
C (15)	69 (2)	67 (2)	38 (1)	-6 (1)	-13 (1)	2 (2)

**Table 6.** Hydrogen-bond geometry ( $\text{\AA}$ ,  $^\circ$ ) of compound 2.

D—H...A	D—H	H...A	D...A	D—H...A
C14—H14...O1 <sup>i</sup>	0.93	2.58	3.482 (4)	164

Symmetry code: (i) 1+x, y, 1+z.

**Figure 4.** Crystal packing of compound 1. Hydrogen atoms are omitted for clarity.**Figure 5.** Crystal packing of compound 2. Hydrogen atoms, except those which involved in hydrogen bonding, are omitted for clarity.**Figure 6.** The  $d_{norm}$  mapped on Hirshfeld surface for visualizing the intermolecular contacts of the compound 1.**Figure 7.** The  $d_{norm}$  mapped on Hirshfeld surface for visualizing the intermolecular contacts of the compound 2.

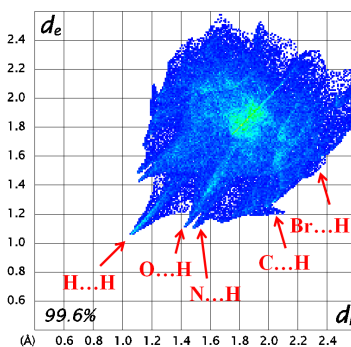


Figure 8. Two-dimensional fingerprint plots of compound 1 shows the 99.6% contacts involved in the crystal packing.

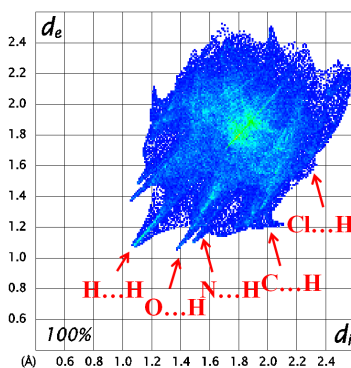


Figure 9. Two-dimensional fingerprint plots of compound 2 shows the 100% contacts involved in the crystal packing.

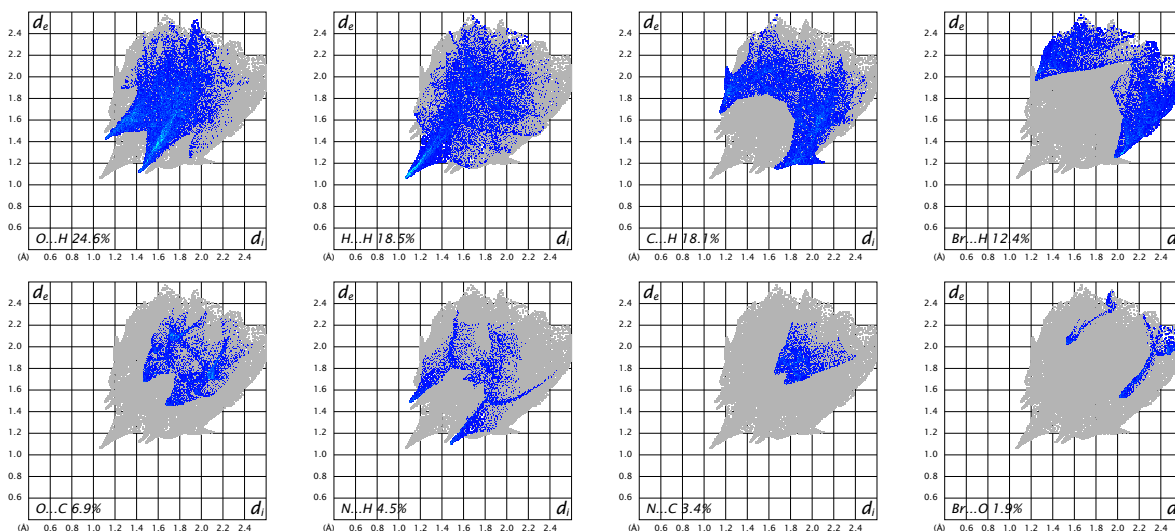


Figure 10. Two-dimensional fingerprint plots indicate the major contributions of intermolecular interactions in compound 1.

The fingerprint plot reveals that the contribution of O...H interaction is 24.6%, to the crystal packing (Figure 12) in compound 1 and 25.1% in compound 2 (Figure 13). Other important interactions for compound 1 are H...H (18.5%), C...H (18.1%), Br...H (12.4%), followed by weak O...C (6.9%), N...C (3.4%), and N...H (4.5%), and for compound 2 are H...H (18.6%), C...H (18.0%), followed by weak O...C (7%), C...C (5.9%), and N...H (4.5%), interactions (Figure 13).

### 3.3. In vitro antileishmanial activity

Compounds 1 and 2 were evaluated for their *in vitro* antileishmanial activity against *Leishmania Major* promastigotes (Table 7) and found as weak antileishmanial agents with  $IC_{50}$  values  $73.2 \pm 3.1$  and  $72.2 \pm 2.3$   $\mu\text{g/mL}$ , respectively against the standard antileishmanial drugs, pentamidine ( $IC_{50} = 5.09 \pm 0.04$   $\mu\text{g/mL}$ ) and amphotericin B ( $IC_{50} = 0.29 \pm 0.05$   $\mu\text{g/mL}$ ).

**Table 7.** Antileishmanial activity of compounds **1** and **2** against *L. Major* promastigotes.

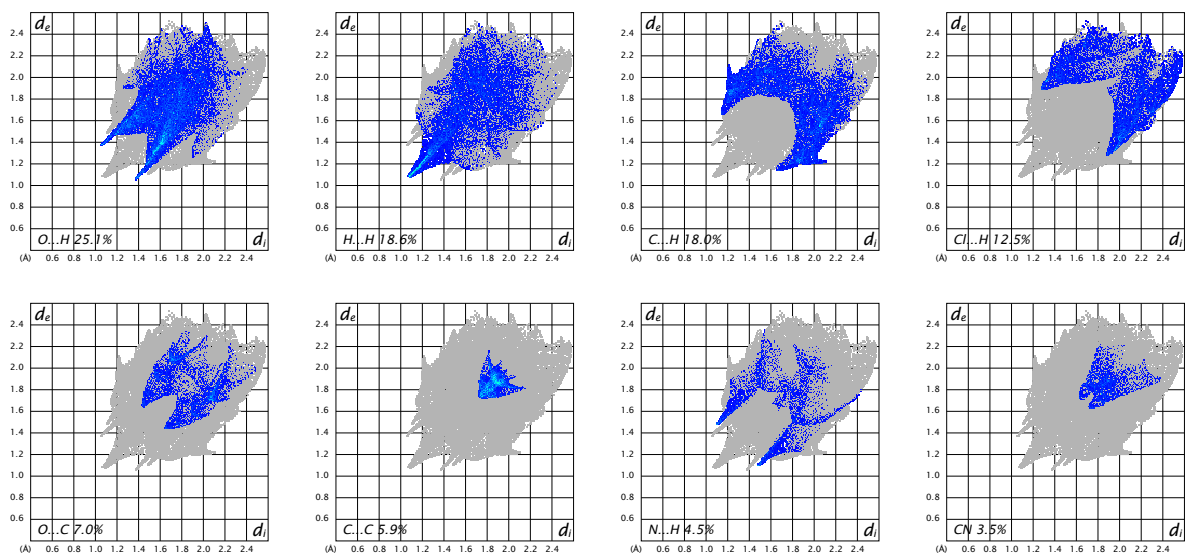
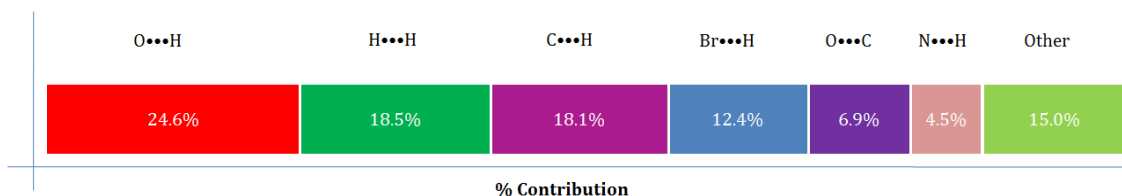
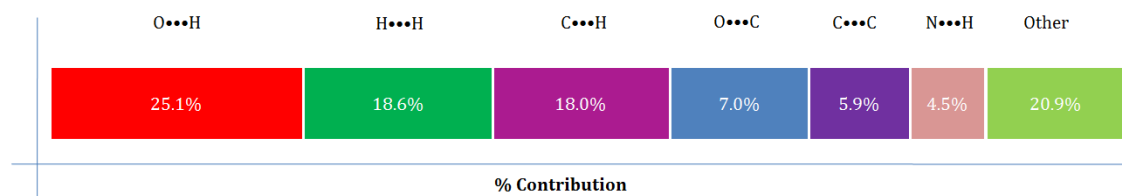
Compounds	IC <sub>50</sub> (μM±SEM) *
<b>1</b>	73.2±3.1
<b>2</b>	72.2±2.3
Pentamidine	5.09±0.09
Amphotericin B	0.29±0.05

\* SEM = Standard error of mean.

**Table 8.** Cytotoxic activity of compounds **1** and **2** against 3T3 fibroblast cell line.

Compounds	Cytotoxicity IC <sub>50</sub> [μM±SD] *
<b>1</b>	8.3±0.4
<b>2</b>	9.4±1.06
Doxorubicin (standard)	0.56±0.15

\* SD = Standard deviation.

**Figure 11.** Two-dimensional fingerprint plots indicate the major contributions of intermolecular interactions in compound **2**.**Figure 12.** The relative contributions to the 99.6% of Hirshfeld surface area for the various intermolecular contacts in compound **1**.**Figure 13.** The relative contributions to the 100% of Hirshfeld surface area for the various intermolecular contacts in compound **2**.

### 3.4. *In vitro* cytotoxic activity

Compounds **1** and **2** were also evaluated for their cytotoxic effect against 3T3 fibroblast cell lines. Both compounds **1** and **2** were found to be cytotoxic in nature with IC<sub>50</sub> values 8.3±0.4 and 9.4±1.06 μg/mL, respectively. Doxorubicin (IC<sub>50</sub> = 0.56±0.15 μg/mL) was used as a standard drug to compare the activity against 3T3 cell line (Table 8).

### 3.5. *In vitro* anti-bacterial activity

The *in vitro* antibacterial activity of compounds **1** and **2** against *E. coli* reference (ATCC25922 and ATCC 35218) and multi-drug resistant (M2 and M3) strains was also investigated. Compounds **1** and **2** exhibited potent anti-bacterial activity against *E. coli* reference cell cultures ATCC 35218 (**1**, 91.42%, **2**, 92.95% inhibition) and ATCC 25922 (**1**, 93.18%, and **2**, 94.5, % inhibition).

**Table 9.** Anti-bacterial activity of compounds **1** and **2** against reference and multi-drug resistant clinical isolates of *E. coli*.

Compounds	% Inhibition			
	ATCC 25922	ATCC 35218	M2	M3
1	91.42	93.18	93.59	93.11
2	92.95	94.5	94.30	94.72
Standards	Ofloxacin = 96.75, Gentamycin = 96.63		Ofloxacin = 0.0, Gentamycin = 97.2	Ofloxacin = 0.0, Gentamycin = 92.07

The activity was found to be comparable to the tested standard drugs, ofloxacin and gentamycin which showed 96.75 and 96.63% inhibition against ATCC 35218 and ATCC 25922 cell cultures, respectively. Similarly both compounds were also appeared as potent anti-bacterial agent against *E. coli* multi-drug resistant clinical isolates M2 (**1**, 93.59 % inhibition, **2**, 94.30 % inhibition) and M3 (**1**, 93.11 % inhibition, **2**, 94.72 % inhibition). The activity was found to be comparable to the tested standard drugs gentamycin which showed 97.20 and 92.07 % inhibition against *E. coli* multi-drug resistant clinical isolates M2 and M3, respectively while ofloxacin was found to be inactive against both M2 and M3 strains. Results are summarized in Table 9.

#### 4. Conclusion

Two new quinoline derivatives **1** and **2** were synthesized, and their three-dimensional structures were deduced by single crystal X-ray diffraction analysis. In the crystal packing of quinoline derivative **2**, two neighboring molecules are interconnected via C-H...O interactions, and the repeating motif of connected molecules arranged along *c* axis. We also calculated the individual molecular interactions in terms of histogram by using Hirshfeld surface analysis and fingerprint plots for compounds **1** and **2** and found that the contribution of O...H intermolecular interactions is more than other (C...H, N...H, etc.) interactions towards crystal stability. The synthesized compounds were found as potent anti-bacterial agents against *E. coli* reference (ATCC25922 and ATCC 35218) and multi-drug resistant strains (M2 and M3) and showed weak anti-leishmanial activity against *L. Major* promastigotes *in vitro*. The synthesized quinoline derivatives were also appeared as cytotoxic in nature against 3T3 fibroblast cell line.

#### Acknowledgments

Dr. Sammer Yousuf is thankful to the Higher Education Commission of Pakistan for the financial support through research fundings 20-2830/R&D/HEC and 20-2216/R&D/HEC.

#### Supplementary data

Crystallographic data for the structure reported in this article have been deposited with Cambridge Crystallographic Data Center, CCDC 1572291 (Compound **1**) and CCDC 1572292 (Compound **2**). Copies of this information may be obtained free of charge from the Director, CCDC, 12 Union Road, Cambridge, CB2 1EZ, UK. Fax: (44)01223336033, E-mail: [deposit@ccdc.cam.ac.uk](mailto:deposit@ccdc.cam.ac.uk) or <http://www.ccdc.com.ac.uk/deposit>.

#### References

- [1]. Solomon, R.; Lee, H. *Curr. Med. Chem.* **2011**, *18*(10), 1488-1508.
- [2]. LaMontagne, M. P.; Markovac, A. M. S.; Sami, K. M. J. *Med. Chem.* **1982**, *25*, 964-968.
- [3]. Denny, W. A.; Wilson, W. R.; Ware, D. C.; Atwell, G. J.; Milbank, J. B.; Stevenson, R. J. US Patent 7064117B2, 2006.
- [4]. Muruganantham, N.; Sivakumar, R.; Anbalagan, N.; Gunasekaran, V.; Leonard, J. T. *Biol. Pharm. Bull.* **2004**, *27*, 1683-1687.
- [5]. Keri, R. S.; Patil, S. A. *Biomed. Pharmacother.* **2014**, *68*(8), 1161-1175.
- [6]. Leatham, P. A.; Bird, H. A.; Wright, V.; Seymour, D.; Gordon A. *Eur. J. Rheumatol. Inflamm.* **1983**, *6*, 209-211.

- [7]. Wilson, W. D.; Zhao, M.; Patterson, S. E.; Wydra, R. L.; Janda, L.; Strekowski, L. *Med. Chem. Res.* **1992**, *2*, 102-110.
- [8]. Strekowski, L.; Mokrosz, J. L.; Honkan, V. A.; Czarny, A.; Cegla, M. T.; Patterson, S. E. *J. Med. Chem.* **1991**, *34*, 1739-1746.
- [9]. Bruker (2009). *SADABS*. Bruker AXS Inc., Madison, Wisconsin, USA.
- [10]. Sheldrick, G. M. *Acta Cryst. A* **2008**, *64*, 112-122.
- [11]. Spek, A. L. *Acta Cryst. D* **2009**, *65*, 148-155.
- [12]. Spek, A. L. *J. Appl. Cryst.* **2003**, *36*, 7-13.
- [13]. Wolff, S.; Grimwood, D.; McKinnon, J.; Turner, M.; Jayatilaka, D.; Spackman, M., *Crystal Explorer*, The University of Western Australia Perth, Australia, 2012.
- [14]. Oxford Diffraction, CrysAlis PRO and CrysAlis RED, Oxford Diffraction Ltd., Abingdon, Oxfordshire, England, 2010.
- [15]. Moreno-Fuquen, R.; Castillo, J. C.; Abonia, R.; Portilla, J.; Henao, J. A. *Molbank* **2017**, *1*, m934-m934.
- [16]. Choudhary, M. I.; Yousuf, S.; Ahmed, S.; Samreen; Yasmeen, K.; Attar-Rahman, *Chem. Biodivers.* **2005**, *2*(9), 1164-1173.
- [17]. Siddiqui, H.; Tasneem, S.; Farooq, S.; Sami, A. Atta-Ur-Rahman; Choudhary, M. I., *Med. Chem.* **2017**, *13*(5), 465-476.
- [18]. Oladimeji, A. O.; Oladosu, I. A.; Ali, M. S.; Khan, S. A.; Yousuf, S. *J. Biol. Activ. Prod. Nat. (TBAP)* **2016**, *6*(5,6), 365-372.